Current Topics in Biophysics 2000, 24(2), 231–240

TISSUE DISTRIBUTION AND DECAY OF TEMPOL AFTER A SINGLE INTRAVENOUS OR INTRAPERITONEAL INJECTION

TOMASZ H. WIERZBA[1*], PAWEŁ MUSIAŁ[2], MACIEJ CHEREK[1], JERZY NOWAK[3], ZBIGNIEW WYPYCH[4]

[1]Department of Physiology, Medical University of Gdańsk,
[2]Department of Animal Physiology, University of Gdańsk,
[3]Department of Biophysics, Medical University of Gdańsk,
[4]Department of General Chemistry, Medical University of Gdańsk

The study was focused on the tissue distribution and decay of a piperidine nitroxide, 4-hydroxy-2,2,6,6-tetramethylpiperidine-N-oxyl (Tempol) in the rat. The experiments were performed on 18 male, Wistar rats. The animals were sacrificed at a given time after the single dose (100 μmol/kg) intravenous or intraperitoneal injection of Tempol. Selected tissues and blood were collected, homogenized in phosphate buffer alone and in combination with benzene and assayed with the electron paramagnetic resonance spectroscopy (ESR) for Tempol. Tempol highly accumulated in plasma and red blood cells, wherein it persisted over 6 hours. Significant triplets of the ESR Tempol peaks were detected in lung, pancreas and heart. Lower, but significant intensity of the Tempol ESR signal was found in brain and soleus muscle, whereas only negligible and transient presence of Tempol was revealed in liver, kidney and testis. As shown by comparison of half-life and the time of 90% decay, the Tempol elimination rate was as follows: red blood cells ≤ plasma < lung < soleus muscle ≤ brain ≤ pancreas ≤ heart < liver < kidney < testis. Monoexponential rate of Tempol decay was observed in heart, soleus muscle and pancreas, whereas its elimination from plasma, red blood cells and lung obeyed the second-order kinetics. In pancreas and kidney Tempol was localized in aqueous compartment, but in lung, liver and testis it appeared predominantly in lipid environment. Prolonged persistence of Tempol in bloodstream and some tissues after a single intravenous or intraperitoneal administration confirms that Tempol not only can serve as a potential research tool for short lasting experiments but also can be of relevant potential in chronic protocols.

INTRODUCTION

Oxidative stress is known to accelerate the generation of reactive oxygen species. Excessive formation of oxygen free radicals is commonly believed to be involved in the development of various pathologies, including ischemic heart disease, atherosclerosis, cancerogenesis, neurodegenerative diseases, radiation injury, skin disorders and arthritis (Evans, 1993; Gutteridge, 1993; Knight, 1995). In recent years several research strategies have been attempted to limit generation of reactive oxygen species or to trap the radicals produced. Nitroxides that can react and eliminate excessively produced oxygen free radicals, such as superoxide anion, have been successfully implemented in the studies on protection of biological systems from oxidative damage (Koerner, Anderson & Dage, 1991; Charloux, Paul, Loisance & Astrier, 1995; Samuni & Barenholz, 1997; Zeltcer, Berenshtein, Samuni & Chevion, 1997). Tempol (4-hydroxy-2,2,6,6-tetramethylpiperidine-N-oxyl) is a representative piperidine nitroxide, which can easily penetrate biological membranes and accumulates both in lipid microenvironment (Timoshin & Ruuge, 1997) and in the cytosolic compartment (Mc Connell, Wright & Mc Farland, 1972). It is somehow peculiar that Tempol and other nitroxides have been as yet employed exclusively in short time experimental protocols, but neither in prolonged studies. The point is, that despite the fact that it has been widely used in research for about three decades, there are still controversies concerning its distribution and kinetics in biological environment (De Zwart, Meerman, Commandeur & Vermeulen, 1998). A short, 2–3 min metabolic half-life of Tempol have been reported in whole rat injected intravenously with Tempol (Matsumoto, Mori, Tsuchihashi, Ogata, Lin, Yokoyama & Ishida, 1998) and in ischemic heart

*Corresponding author: Tomasz Wierzba, Department of Physiology, Medical University of Gdańsk, 80–211 Gdańsk, Dębinki 1, Poland; tel.: +48 (58) 3491520; e-mail: twierzba@amg.gda.pl

(Kuppusamy, Chzhan, Vij, Shteynbuk, Lefer, Gianella & Zweier, 1994). Much longer Tempol persistence, with the half-life ranging from 22 to 60 min have been shown in the isolated heart (Rosen, Halpern, Brunsting, Spencer, Strauss, Bowman & Wechsler, 1988; Kuppusamy, Wang, Zweier, Krishna, Mitchell, Ma, Trimble & Hsia, 1996), cultured cells (Hahn, Krishna, Samuni, De Graff, Cuscela, Johnstone & Mitchell, 1994) and whole mice (Twomey, Taira, De Graff, Mitchell, Russo, Krishna, Hankovszky, Frank & Hideg, 1997). The reported discrepancies might result from different accuracy of electron parametric resonance spectroscopy (ESR) employed in particular studies and from different experimental procedures applied. It is well known that the major way of Tempol decay is its reduction to the corresponding diamagnetic, ESR silent hydroxylamine. The mechanism of this reduction depends upon several factors, such as oxygen concentration (Chen, Glockner, Morse & Swartz, 1988), ascorbate and glutathione, vitamin E concentration (Głębska & Gwoździński, 1998; Matsumoto *et al.*, 1998), transition metals (Zeltcer *et al.*, 1997) and the rate of reoxidation of the hydroxylamine (Samuni, Krishna, Mitchell, Collins & Russo, 1990).

The present study was focused on the tissue distribution and kinetics of Tempol after its single intravenous, or intraperitoneal administration in the normal adult rat.

MATERIAL AND METHODS

Chemicals

4-hydroxy-2,2,6,6-tetramethylpiperidine-N-oxyl (Tempol) was synthesized as described by Rozantsev (1970). Purity of at least 99.9% was confirmed by precise estimation of the melting point. All other reagents were of analytical grade.

Animals

The experiments were performed on 18 male Wistar 16-weeks-old rats (350–430 g), divided randomly into 2 groups. The rats were housed in individual cages at 24 ± 2°C. A 12-h light/12-h dark cycles and free access to a standard diet and water was provided. The experimental protocol was reviewed and approved by the local Institutional Ethics Committee.

Tempol dosage

The day before the proper experiment, the rats of the group preselected for intravenous Tempol injection were surgically instrumented under mild ethyl ether anesthesia. The polyethylene tubing PE-50 (Beckton-Dickinson, USA) was introduced into the left jugular vein and exteriorized subcutaneously at the back of the neck. The second group of animals enrolled for intraperitoneal dosage remained intact at that time. The next day all animals were injected with Tempol (100 μmol/kg) dissolved in isotonic saline. The dose was administered intravenously or intraperitoneally, depending on the group. Then, at the exact moment after the injection (5, 15, 30, 60, 180 and 360 min) the rats were sacrificed by decapitation. A 2–3 ml sample of blood was collected into a heparinized vial. The heart, lung, brain, liver, pancreas, kidney, testis and soleus muscle were rapidly excised and washed in phosphate-buffered saline (PBS, pH = 7.4) and their wet weight was determined.

Sample preparation

Blood was centrifuged for 10 min at 1400 rpm. Red blood cells and plasma were separated. Red blood cell suspension was divided into 2 parts. The first aliquot was left to represent both hydrophilic and lipid cellular compartments. Benzene was added to the second one (1:3 vol/vol) to assess lipid fraction of the cells. Then, the sample was carefully stirred, incubated for 30 min at room temperature, stirred again, and centrifuged for 10 min at 1400 rpm. The benzene fraction of the supernatant was extracted for further analysis. All tissues were homogenized in PBS buffer to give 15% tissue homogenate, which was subsequently aliquoted into the intact PBS homogenate and benzene (1:3 vol/vol) treated samples. The following procedure was identical as in case of red blood cells.

Tempol assay

Plasma, red blood cell suspension, and tissue homogenates were assayed for Tempol. The quartz capillary was filled with 150 μl of the sample and placed in the resonator chamber of the VARIAN E-4 ESR spectrometer. The scanning parameters were: scan time 1 min, modulation amplitude 5 G, microwave power 20 mW, microwave frequency 9.55 GHz, receiver gain 2.5×10^1 to 2×10^4, scan width 100 G, scan center 3380 G, time constant 0.3 s (tissue samples) or 1 s (blood samples), room temperature (22°C). Every scan was digitized and repeated 4 times. The average ESR signals were recorded following the combined computer analysis of the scans. The resolving power and precision of the ESR assay was increased by subtraction of signals received from the homogenate-filled samples from the signals obtained from quartz capil-

lary filled with pure PBS. Using the above method in a pilot study, we were able to record the unique ESR spectra of Tempol from its 100 nM solutions in PBS homogenates of rat myocardium.

Data analysis

Tempol content in the tested samples was confirmed by recording of the unique triplet ESR spectra. Since the receiver gain was fluently adjusted to the height of the obtained Tempol spectra, increasing when the peaks of the Tempol spectrum were low, the noise signal was not constant. The higher gain adjusted resulted with increase in noise. The magnitude of the middle peak of the Tempol spectra was used for quantitative analysis. The noise amplitude was assessed using as the highest value of moving average calculated in each scan from 40 (20 in case of blood samples) single ESR data acquisitions (at time constant of 0.3 s). The ratio signal (height of the middle peak of the Tempol spectrum) to noise (average amplitude of the background) was computed and employed as an index of signal intensity related to Tempol concentration in tested samples. The average value of the signal/noise ratio from different rats was calculated from a given kind of sample data (e.g. PBS heart homogenate, plasma) at the same time after the injection of Tempol. Natural logarithm of signal to noise intensity ratio (ln S/N) was plotted against time. The characteristics of tissue decay of Tempol was revealed with analysis of trend using Tool Pack Analysis software package from Microsoft Excel. The method is based on the least square fitting of the observed intensity data to a function. Half-life of Tempol ($t_{1/2}$) and time of 90%decay ($t_{9/10}$) was estimated from the received function formula. Microsoft Excel software was also employed for calculation of the signal and the noise amplitude and their ratio.

RESULTS AND DISCUSSION

Representative spectra of the tested samples are shown in Fig. 1. The important finding is that resonance line width was practically identical in all scans. Since the line width is proportional to oxygen concentration and is a sensitive marker of ischemia (Rosen *et al.*, 1988; Zweier & Kuppusamy, 1988; Chen *et al.*, 1989), we assumed that in our study oxygen conditions were similar in all samples. It is crucial for comparison of the intensity of Tempol signal among tissues, since theoretically Tempol could have been restored from the ESR silent hydroxylamine in excess of oxygen (Samuni *et al.*, 1990), which could have been introduced into samples during the homogenization procedure. On the other hand, since the both compounds have been recently shown to be protective in oxidative stress (Zhang, Pinson & Samuni, 1998), the source of Tempol, direct, from injection *in vivo*, or indirect, as a result of hydroxylamine oxidation does not seem to be of vital importance.

It is not fully clear what is the minimum value of S/N ratio necessary for the reliable detection of Tempol. It is generally accepted that it should exceed 1 (Matsumoto *et al.*, 1998). However, in

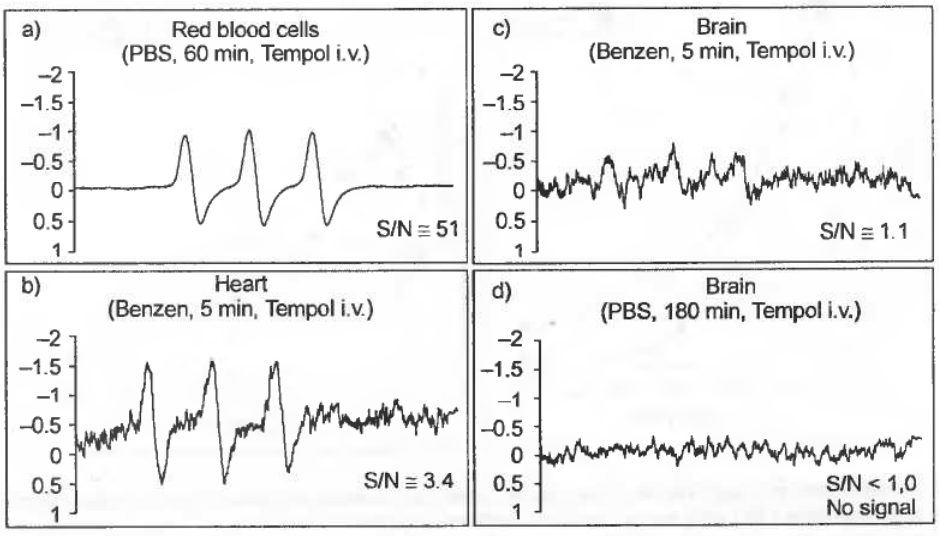

Fig. 1. Representative ESR spectra from the tested tissues and blood samples

case of implementing high gain (10^4), or even higher, the noise signal is sometimes irregular and in some cases it is possible to recognize the unique shape of Tempol spectra at S/N ratio lower than 1. To provide validity of the assay we arbitrarily regarded the S/N ratio lower than 1.1 ($\ln < 0.1$) as insignificant.

The kinetics of Tempol in tissues after its intravenous or intraperitoneal injection is visualized in Figures 2–5. The prominent triplet Tempol signal was clearly seen with excellent signal/noise (S/N) ratios of > 400 in plasma and red blood cell samples, within the first 15 min after the intravenous Tempol injection. Following the intraperitoneal dosage a substantial ESR Tempol spectra appeared as well. However, the intensity of the signal (S/N) was lower by about one order of magnitude compared to the intravenous injection. Noteworthy, Tempol persisted in the bloodstream over 4 hours after the intraperitoneal dose and about 7 hours

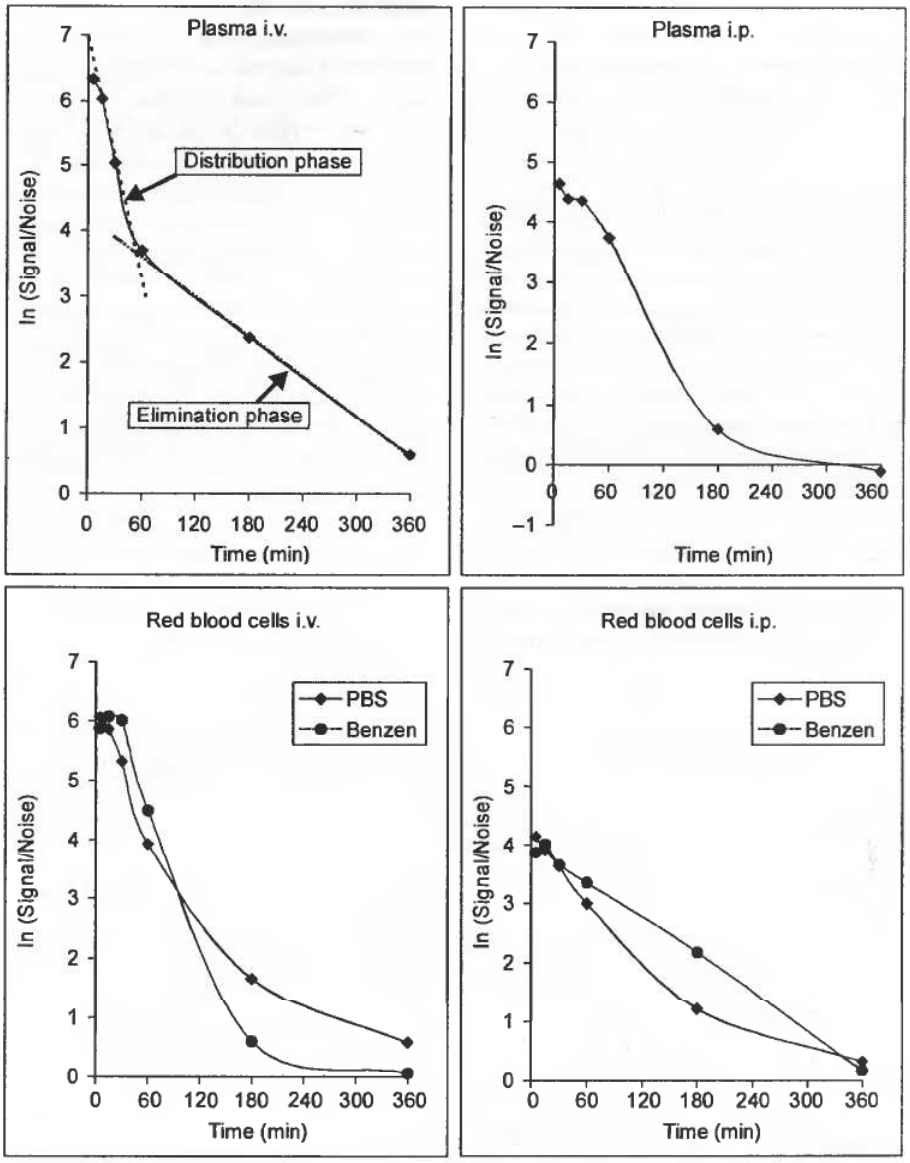

Fig. 2. Semilogarithmic plot illustrating the decrease in the Tempol signal intensity in plasma and red blood cells, expressed as a ln of signal/noise (S/N) ratio, against time after intravenous injection of Tempol (100 μmol/kg). Values of ln S/N < 1.1 were regarded arbitrarily as insignificant and marked with as a shaded area. Each point represents mean value of 2 to 3 samples

after the intravenous injection as extrapolated from the decay curve. Significant triplets of the ESR Tempol peaks were detected in lung, pancreas and heart. Lower intensity of the Tempol ESR signal was found in brain and soleus muscle, whereas only negligible and transient presence of Tempol could be seen in liver, kidney and testis. Tissue absorption pattern was non uniform, depending on the way of administration and on the tissue. Maximal amplitude of the Tempol ESR spectra was observed within 5 min after its intravenous or intraperitoneal administration in the heart and plasma and also in PBS homogenates of pancreas after the iv. dose. In red blood cell samples as well as in the majority of homogenates of lung, soleus muscle, pancreas (lipid fraction), liver (lipid fraction) the peak concentration of Tempol was revealed within 15 min. More prolonged Tempol accumulation, lasting up to 30 min after its administration was observed in brain, lipid fraction

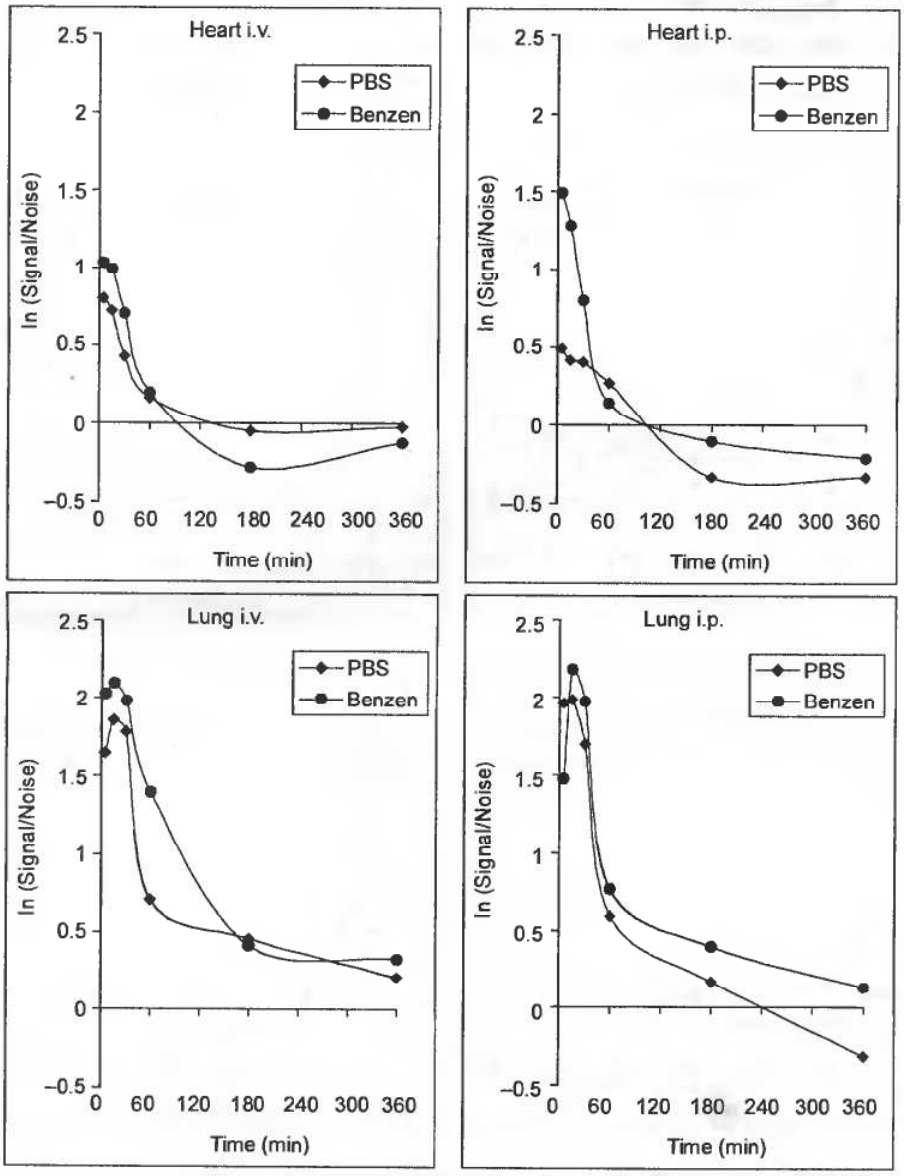

Fig. 3. Semilogarithmic plot illustrating the decrease in the Tempol signal intensity in homogenates obtained from heart and lung, expressed as a ln of signal/noise (S/N) ratio, against time after intravenous injection of Tempol (100 μmol/kg). Values of ln S/N < 1.1 were regarded arbitrarily as insignificant and marked with as a shaded area. Each point represents mean value of 2 to 3 samples

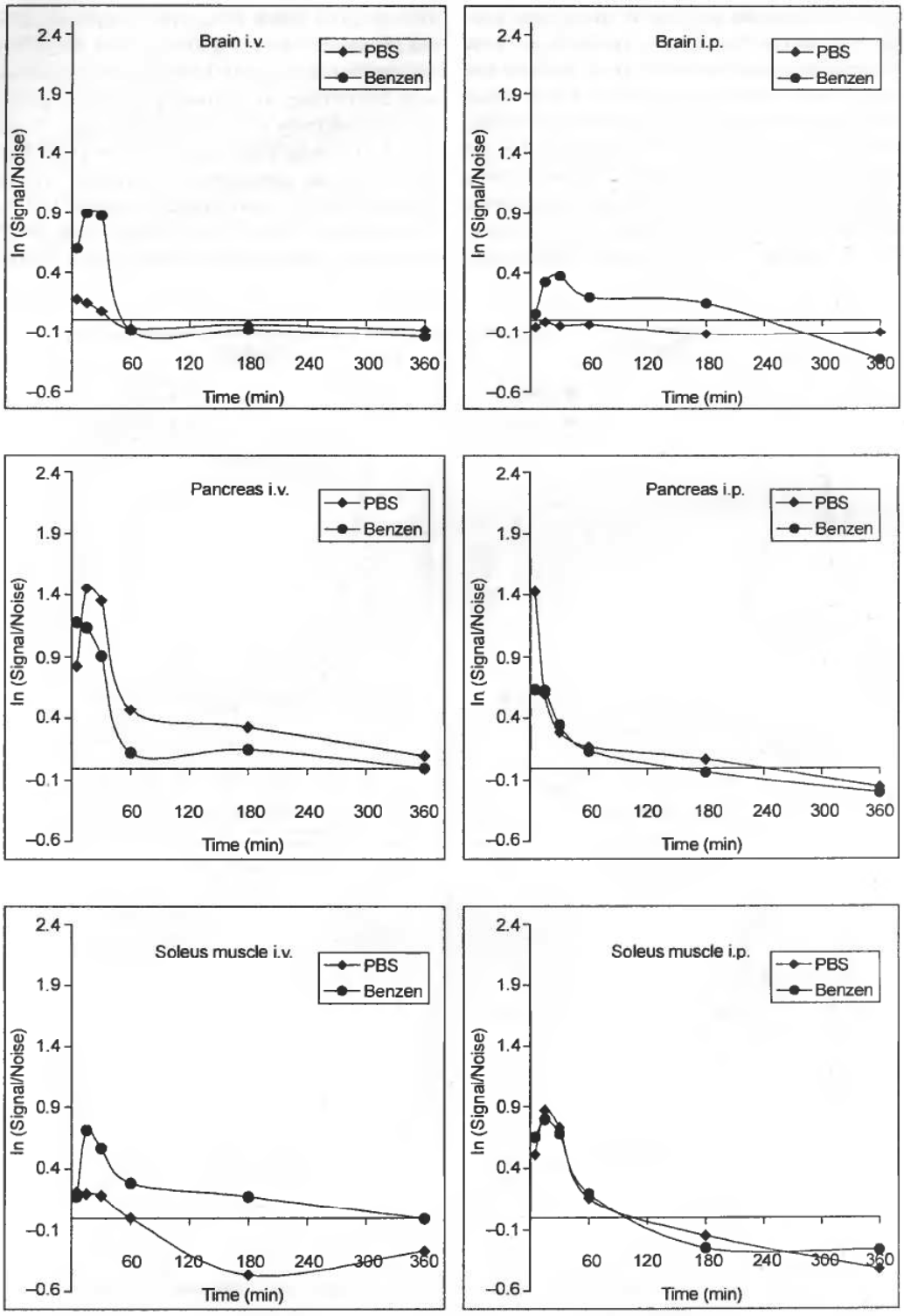

Fig. 4. Semilogarithmic plot illustrating the decrease in the Tempol signal intensity in homogenates obtained from brain, pancreas and soleus muscle, expressed as a ln of signal/noise (S/N) ratio, against time after intravenous injection of Tempol (100 μmol/kg). Values of ln S/N < 1.1 were regarded arbitrarily as insignificant and marked with as a shaded area. Each point represents mean value of 2 to 3 samples

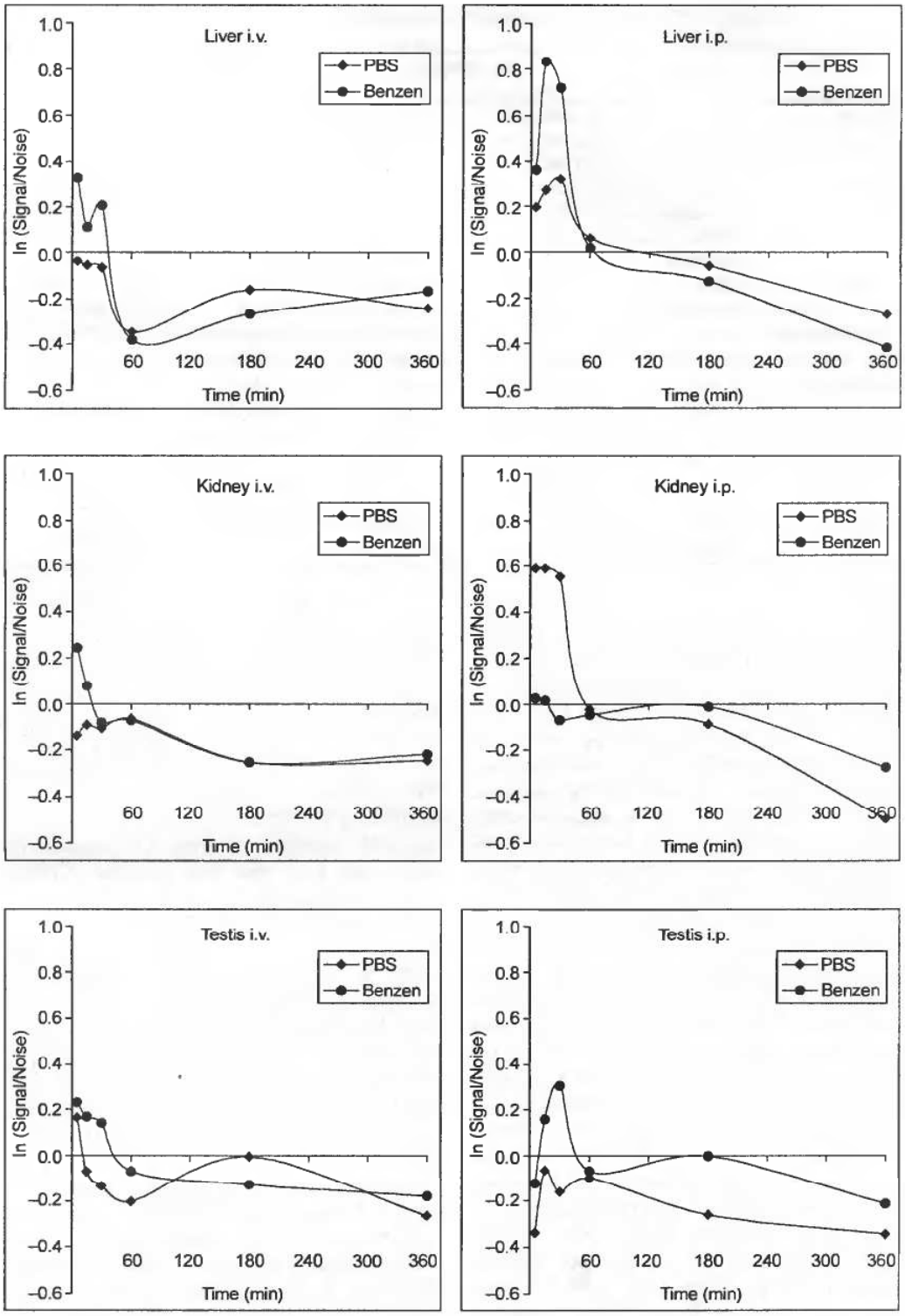

Fig. 5. Semilogarithmic plot illustrating the decrease in the Tempol signal intensity in homogenates obtained from liver, kidney and testis, expressed as a ln of signal/noise (S/N) ratio, against time after intravenous injection of Tempol (100 μmole/kg). Values of ln S/N < 1.1 were regarded arbitrarily as insignificant and marked with as a shaded area. Each point represents mean value of 2 to 3 samples

Table 1. Tempol half-life and time of its 90% decay in the tested tissues

Tissue	Sample	$t_{1/2}$ (min)		$t_{9/10}$ (min)	
		i.v.	i.p	i.v.	i.p.
Plasma	Intact	93	110	337	189
Red blood cells	PBS	96	189	375	340
	Benzene	96	198	363	355
Heart	PBS	29	76	91	96
	Benzene	39	31	76	60
Lung	PBS	45	48	195	179
	Benzene	93	43	245	348
Brain	PBS	28	not available	39	not available
	Benzene	37	158	45	226
Soleus muscle	PBS	42	39	56	80
	Benzene	45	40	210	93
Pancreas	PBS	41	12	187	115
	Benzene	37	25	not available	not available
Liver	PBS	not available	40	not available	48
	Benzene	31	38	36	71
Kidney	PBS	not available	38	not available	51
	Benzene	12	16	19	18
Testis	PBS	8	not available	11	not available
	Benzene	34	36	40	45

of testis, PBS homogenates of pancreas (Tempol i.v.) and kidney (Tempol i.p.). In the lung, liver and testis Tempol accumulated predominantly in the lipid environment, whereas in the kidney and pancreas it was preferably localized within the aqueous compartment. The latter observation may suggest that Tempol is released into the pancreatic juice and urine, but rather not accumulated within the cellular compartment of the both organs. Tempol half-life and time of its 90% decay in the tested tissues are shown in Table 1. Time course of the Tempol reduction in the tested samples was found to be heterogeneous (Fig. 2–5). Monoexponential decay, which is referred to the first-order kinetics was observed in the heart, soleus muscle and pancreas, whereas it obeyed the second order kinetics in the plasma, lung and red blood cells. In the other tissues assayed: kidney, liver, testis and brain the kinetic model has not been established since Tempol accumulation was too low and the Tempol ESR spectra disappeared rapidly. Tissue elimination of the piperidine nitroxides has been frequently reported as the simplest, one-phase exponential decay (Giotta & Wang, 1972; Stier & Sackmann , 1973; Berliner & Wan, 1989; Iannone, Tomasi, Vanini & Swartz, 1990; Alecci, Ferrari, Quaresima, Sotgiu & Ursini, 1994; Komarov, Joseph & Lai, 1994; Krishna, Samuni, Taira, Goldstein, Mitchell & Russo, 1996; Twomey *et al.*, 1997; Głębska & Gwoździński, 1998; Togashi, Matsuo, Shinzawa, Takeda, Shao, Oikawa, Kamada & Takahashi, 2000). The impact of these studies is limited by the methods used and their restrictions: a short time of ESR assay not exceeding 30 minutes, or low sensitivity of ESR detection due to a relatively big sample volume placed into a resonator chamber, or by using *ex vivo* experimental models such as cultured cells or microsomal membranes. More complex models of nitroxide depletion, obeying the second-order kinetic rate have been also described (Griffeth, Rosen, Rauckman & Drayer, 1984; Rosen *et al.*, 1988; Samuni, Krishna, Riesz, Finkelstein & Russo, 1989; Vianello, Momo, Scarpa & Rigo, 1995). Mechanisms underlying the complexity of the nitroxide decay rate under *in vivo* condition have been already pointed out: disequilibrium between the rate of nitroxide reduction to the corresponding hydroxylamine and the rate of intracellular penetration where this reduction undergoes (Swartz, Sentjurc & Morse, 1986), different ability of particular tissues to quench and reduce nitroxides (Masumizu, Kohno & Nakata, 1999), metabolic status of particular tissue related to age or tissue damage (Inaba, Nakashima, Shima, Mitsuyoshi, Sakamoto, Okanue, Kashima, Hashiba, Nishikawa & Watari, 1997; Nishino, Yasui & Sakurai, 1999) and physical interaction with red blood cell membranes and plasma albumins (Bennett, Brown, Keana, Koenog & Swartz, 1990). In this regard, our finding, based on prolonged ESR assay, that in plasma and red blood cells and also

in some tissues such as lung, Tempol elimination does not obey a monoexponential decay, but that more complex mechanisms are involved, where phases of distribution and elimination can be distinguished, seems to be important and put a new insight into the studies on the nitroxide kinetics in biological systems.

In majority of scans, the signal to noise ratio (S/N) did not exceed 4 (ln S/N = 1.39), ranging between 1.5 and 3 (ln S/N between 0.4 and 1.1). The unique Tempol spectrum could be recognized by its shape and the exact magnetic field position. This relatively low Tempol signal corresponds to the Tempol tissue concentration of 0.1–1 μM as estimated from the preliminary data. Our concentration evaluation is consistent with the study of Zweier and Kuppusamy (1988) in which they detected the characteristic nitroxide spectra in aqueous 400 nM samples. The prime condition for the radical scavenger to eliminate radicals generated in biological systems is its presence on the spot, provided by an appropriate dosage. It has been reported that oxygen free radicals are generated in 0.1–1 μM concentrations on reperfusing ischemic tissues (Zweier, Flaherty & Weisfeld, 1987), which is comparable to the Tempol tissue concentration obtained after a single dosage. Since reaction of Tempol with its major free radical substrate, superoxide anion, proceeds in a stoichiometric mode, it is likely that it may indeed provide a substantial protection from oxidative damage.

CONCLUDING REMARKS

Tissue distribution and kinetics of Tempol decay, and in particular, its long persistence in the bloodstream after single intravenous or intraperitoneal administration confirms that this compounds can not only serve as a potential research tool for short lasting experiments but also be of value in more prolonged studies.

REFERENCES

Alecci M., Ferrrari M., Quaresima V., Sotgiu A. & Ursini C. L. (1994). Simultaneous 280 MHz EPR imaging of rat organs during nitroxide free radical clearance. *Biophys. J.*, **67**, 1274–1279.

Bennett H. F., Brown R. D., Keana J. F., Koenog S. H. & Swartz H. M. (1990). Interactions of nitroxide with plasma and blood: effect on 1/T1 of water protons. *Magn. Reson. Med.*, **14**, 40–55.

Berliner L. J. & Wan X. M. (1989). *In vivo* pharmacokinetics by electron magnetic resonance spectroscopy. *Magn. Reson Med.*, **9**, 430–434.

Charloux C., Paul M., Loisance D. & Astrier A. (1995). Inhibition of hydroxyl radical production by lactobionate, adenine, and Tempol. *Free Radic. Biol. Med.*, **19**, 699–704.

Chen K., Glockner J. F., Morse P. D. & Swartz H. M. (1989). Effects of oxygen on the metabolism of nitroxide spin labels in cells. *Biochemistry*, **28**, 2501–2509.

De Zwart L. L., Meerman J. H. N., Commandeur J. N. M. & Vermeulen N. P. E. (1998). Biomarkers of free radical damage application in experimental animals and in humans. *Free Radic. Biol. Med.*, **26**, 202–226.

Evans P. H. (1993). Free radicals in brain metabolism and pathology. *Br. Med. Bull.*, **49**, 577–587.

Giotta G. J. & Wang H. H. (1972). Reduction of nitroxide free radicals by biological materials. *Biochem. Biophys. Res. Commun.*, **46**, 1576-1580.

Głębska J. & Gwoździński K. (1998). Oxygen-dependent reduction of nitoxides by ascorbic acid and glutathione. An EPR study. *Curr. Topics Biophys.*, **22**, (suppl. B), 75–82.

Griffeth L. K., Rosen G. M., Rauckman E. J. & Drayer B. P. (1984). Pharmacokinetics of nitroxide NMR contrast agents. *Invest. Radiol.*, **19**, 553–562.

Gutteridge J. M. C. (1993). Free radicals in disease processes: A compilation of cause and consequence. *Free Radic. Res. Commun.*, **19**, 141–158.

Hahn S. M., Krishna C. M., Samuni A., DeGraff W., Cuscela D. O., Johnstone P. & Mitchell J. B. (1994). Potential use of nitroxides in radiation oncology. *Cancer Res.*, **54**, (suppl), 2006s–2010s.

Iannone A., Tomasi A., Vanini V. & Swartz H. M. (1990). Metabolism of nitroxide spin labels in subcellular fraction of rat liver. Reduction by micrososmes. *Biochem. Biophys. Acta*, **1034**, 285–289.

Inaba K., Nakashima T., Shima T., Mitsuyoshi H., Sakamoto Y., Okanue T., Kashima K., Hashiba M., Nishikawa H. & Watari H. (1997). Hepatic damage influences the decay of nitroxide radicals in mice – an *in vivo* ESR study. *Free Radic. Res.*, **27**, 37–43.

Knight J. A. (1995). Diseases related to oxygen-derived free radicals. *Ann. Clin. Lab. Sci.*, **25**, 111–121.

Koerner J. E., Anderson B. A. & Dage R. C. (1991). Protection against postischemic myocardial dysfunction in anesthetized rabbits with scavengers of oxygen-derived free radicals: superoxide dismutase plus catalase, N-2-mercaptopropionyl glycine and captopril. *J. Cardiovasc. Pharmacol.*, **17**, 185–191.

Komarov A. M., Joseph J. & Lai C. S. (1994). *In vivo* pharmacokinetics of nitroxides in mice. *Biochem. Biophys. Res. Commun.*, **201**, 1035–1042.

Krishna M. C., Samuni A., Taira J., Goldstein S., Mitchell J. B. & Russo A. Stimulation by nitroxides of catalase-like activity of hemoproteins. *J. Biol. Chem.*, **271**, 26018–26025.

Kuppusamy P., Chzhan M., Vij K., Shteynbuk M., Lefer D. J., Gianella E. & Zweier J. L. (1994). *Proc. Natl. Acad. Sci. USA*, **91**, 3388–3392.

Kuppusamy P., Wang P., Zweier J. L., Krishna M. C., Mitchell J. B., Ma L., Trimble C. E. & Hsia C. J. C. (1996). Electron spin resonance imaging of rat heart with nitroxide and polynitroxyl-albumin. *Biochemistry*, **35**, 7051–7057.

Masumizu T., Kohno M. & Nakata M. (1999). Distribution of nitroxide radical compounds and its reducing activity in liver, speen and kidney of rat by electron spin resonance spectroscopy. *Yakugaku Zasshi (English abstract)*, **119**, 956–963.

Matsumoto S., Mori N., Tsuchihashi N., Ogata T., Lin Y., Yokoyama H. & Ishida S. (1998). Enhancement of nitroxide-reducing activity in rats after chronic administration of vitamin E, vitamin C, and idebenone examined by an *in vivo* electron spin resonance technique. *Magn. Reson. Med.*, **40**, 330–333.

Mc Connell H. M., Wright K. L. & Mc Farland B. G. (1972). The fraction of the lipid in a biological membrane that is in a fluid state: a spin label assay. *Biochem. Biophys. Res. Commun.*, **47**, 273–281.

Nishino N., Yasui H. & Sakurai H. (1999). *In vivo* L-band ESR and quantitative pharmacokinetics analysis of stable spin probes in rats and mice. *Free Radic. Res.*, **31**, 35–51.

Rosen G. M., Halpern H. J., Brunsting L. A., Spencer D. P., Strauss K. E., Bowman M. K. & Wechsler A. S. (1988). Direct measurement of nitroxide pharmacokinetics in isolated heart situated in a low frequency electron spin resonance spectrometer: implications for spin trapping and *in vivo* oximetry. *Proc. Natl. Acad. Sci. USA*, **85**, 7772–7776.

Rozantsev E. G. (1970). *Free Nitroxyl Radicals*. Plenum Press, New York.

Samuni A., Krishna C. M., Ries P., Finkelstein E & Russo A. (1989). Superoxide reaction with nitroxide spin-adducts. *Free Radic. Biol. Med.*, **6**, 141–148.

Samuni A. M., Krishna C. M., Mitchell J. B., Collins C. R. & Russo A. (1990). Superoxide reactions with nitroxides. *Free Radic. Res. Commun.*, **9**, 241–249.

Samuni A. M. & Barenholz Y. (1997). Stable nitroxide radicals protect lipid acyl chains from radiation damage. *Free Radic. Biol. Med.*, **22**, 1165–1174.

Stier A. & Sackmann E. (1973). Spin labels as enzyme substrates. Heterogeneous lipid distribution in liver microsomal membranes. *Biochim. Biophys. Acta*, **311**, 400–408.

Swartz H. M., Sentjurc M. & Morse P. D. (1986). Cellular metabolism of-soluble nitroxides: effects on rate of reduction of cell/nitroxide ratio, oxygen concentrations and permeability of nitroxides. *Biochim. Biophys. Acta*, **888**, 82–90.

Timoshin A. A. & Ruuge E. K. (1994) Interaction of rat myocardial tissue with nitroxide radicals. *Biofizika*, **39**, 709–712.

Togashi H., Matsuo T., Shinzawa H., Takeda Y., Shao L., Oikawa K., Kamada H. & Takahashi T. (2000). *Ex vivo* measurement of tissue distribution of a nitroxide radical after intravenous injection and its *in vivo* imaging using a rapid scan ESR-CT system. *Magnet. Reson. Imaging*, **18**, 151–158.

Twomey P., Taira J., De Graff W., Mitchell J. B., Russo A., Krishna M. C., Hankovszky O. H., Frank L. & Hideg K. (1997). Direct evidence for *in vivo* nitroxide free radical production from a new antiarrhythmic drug by EPR spectroscopy. *Free Radic. Biol. Med.*, **22**, 909–916.

Vianello F., Momo F., Scarpa M. & Rigo A. (1995). Kinetics of nitroxide spin label removal in biological systems: an *in vitro* and *in vivo* ESR study. *Magn. Reson. Imaging*, **13**, 219–226.

Zeltcer G, Berenshtein E, Samuni A & Chevion M. (1997) Nitroxide radicals prevent metal-aggravated reperfusion injury in isolated rat heart. *Free Radic. Res.*, **27**, 627–635.

Zhang R., Pinson A. & Samuni A. (1998). Both hydroxylamine and nitroxide protect cardiomyocytes from oxidative stress. *Free Radic. Biol. Med.*, **24**, 66–75.

Zweier J. L., Flaherty J. T. & Weisfeldt M. L. (1987). *Proc. Natl. Acad. Sci. USA*, **84**, 1404–1407.

Zweier J. L. & Kuppusamy P. (1988). Electron paramagnetic resonance measurements of free radicals in the intact beating heart: a technique for detection and characterization of free radicals in whole biological tissues. *Proc. Natl. Acad. Sci. USA*, **85**, 5703–5707.